C. R. Chimie 14 (2011) 1122–1127

Contents lists available at ScienceDirect

Comptes Rendus Chimie

www.sciencedirect.com

Account/Revue

A novel one step synthesis of silver nanoparticles using room temperature ionic liquid and their biocidal activity

R.S. Patil, M.R. Kokate, P.P. Salvi, S.S. Kolekar *

Department of Chemistry, Shivaji University, Kolhapur 416 004 (M.S.), India

ARTICLE INFO

Article history:
Received 4 May 2011
Accepted after revision 21 July 2011
Available online 26 August 2011

Keywords:
Silver nanoparticles
Ionic liquid
Surface plasmon resonance
TEM
Bactericidal activity

ABSTRACT

This article reports the synthesis of silver Nan particles (SNPs) using 1-(dodecyl) 2 amino-pyridinium bromide ionic liquid. This is a new one phase method for the synthesis of uniform monodispersed crystalline silver nanoparticles in a water-ionic liquid system. In this work, the functionalized room temperature IL acts as stabilizing agent and solvent. Hydrazine hydrate acts as reducing agent. To the best of our knowledge, there is no report of the synthesis of metal nanoparticles using this ionic liquid. The synthesis of silver nanoparticles is very primarily studied by UV-Visible spectroscopic analysis. The TEM and particle size distribution was used to study morphology and size of the particles. The charge on synthesized SNPs was determined by Zeta potential. The silver nanoparticles have been known to have inhibitory and bactericidal effect. The investigation of antibacterial activities of ionic liquid stabilized silver nanoparticles was performed by measurement of the minimum inhibitory concentration.

© 2011 Académie des sciences. Published by Elsevier Masson SAS. All rights reserved.

1. Introduction

Ionic liquids have been mainly considered as new reaction media, as catalysts, and as electrolytes for various battery systems because of their unique electrochemical and physical properties [1,2]. Recently, considerable research on nanomaterials has been attempted for room temperature ionic liquids (RTILs) because RTILs generally feature a good stability to air and water, a wide liquid range and unique stability properties to various organic and inorganic substances [3–5]. ILs are ionic compounds with relatively low melting point. They are characterized by very low vapor pressure and consequently, are considered as environmentally benign solvents. In addition, ILs possess interesting properties such as tunable polarity, Lewis acidity, coordinating ability, hydrophilic and miscibility with various compounds [6–8].

Ionic liquids have been used in the synthesis of nanostructured materials, and identification of appropriate surface capping agent in these new solvents remains an important issue. Several currently used capping agents tend to causes irreversible aggregation of nanoparticles [9,10]. Reverse microemulsions are mostly transparent, isotropic and thermodynamically stable liquid media with nanosized water droplets dispersing in continuous oil phase and stabilized by an adsorbed surfactant film at the liquid–liquid interface [11].

Nanoparticles have a wide range of applications in the field of environmental pollution control, drug delivery systems, material chemistry and so on [12]. There has been extensive research in chemical synthesis of nanoparticles. The chemical synthesis of nanoparticles has several occupational exposure hazards like carcinogenicity, genotoxicity, cytotoxicity and general toxicity [13]. Silver is chosen in part because of its size dependent surface plasmon and other unique properties, which have found increasingly broad applications [14–16]. Generally, metal nanoparticles can be prepared by both physical and chemical methods; however, the chemical approach, such

* Corresponding author.
E-mail address: kolekarss2003@yahoo.co.in (S.S. Kolekar).

1631-0748/$ – see front matter © 2011 Académie des sciences. Published by Elsevier Masson SAS. All rights reserved.
doi:10.1016/j.crci.2011.07.009

as reduction, is most widely used [17,18]. The recent advances in research on metal nanoparticles appear to revive the use of silver nanoparticles for antibacterial applications. It has been shown that silver Nan particles (SNPs) prepared with a variety of synthetic methods have effective antimicrobial activity [19–27]. Hence, silver SNPs have been applied to wide range of healthcare products, such as burn dressings, scaffolds, water purification systems and medical devices [28,29].

The interest towards preparation of such hybrid materials is driven by their possible application in the biomedical field as antibacterial coating material or in the electrochemical biosensor field as a catalytically active membrane for direct electron transfer [30]. In conclusion, combined results suggested that SNPs may damage the structure of bacterial enzymes, which cause bacterial cells to die eventually. All studies have shown that the size morphology, stability and properties of metal nanoparticles are strongly influenced by experimental conditions, the kinetics of interaction of metal ion with reducing agent, and adsorption process of stabilizing agent with metal nanoparticles. Hence the design of the synthetic pathway in which the properties of nanoparticles are well controlled has become a major field of interest.

In this study, the synthesis of SNPs is done using a simple RTIL which is newly synthesized and which acts as a stabilizing agent and hydrazine hydrate as reducing agent. The role of the ionic liquid stems from the fact that the thermodynamically driven spontaneous process of nanoparticles agglomeration can be prevented. The reducing ability depends on the concentration of reducing agent. Thus by optimizing the experimental conditions such as silver ion concentration, IL concentration, hydrazine concentration, time, monodispersed silver nanoparticles with high antibacterial activity could be obtained.

2. Experimental

2.1. Materials

The chemicals such as silver nitrate, hydrazine hydrate, 1-bromododecane, 2-amino pyridine were obtained from Merck India. All materials were used without further treatment.

The nutrient agar, Type 1 agar and sodium chloride was purchased from Hi-media. These agars were used to grow and maintain the bacterial culture.

2.2. Synthesis of 2-amino-1-dodecylpyridinium bromide

To a stirred solution of 2-amino pyridine (10 mmol) in ethanol (10 mL), 1-bromodo-decane (15 mmol) was added (Scheme 1). The reaction mixture was stirred at 60–65 °C for 48 h. The formed solid product was washed repeatedly with ethyl acetate, filtrated to remove non-ionic residues and dried in vacuum to get the product 2-amino-1-dodecylpyridinium, bromide. The NMR spectroscopic data is used to confirm the formation of ionic liquid.

NMR Data

^{1}H NMR (300 M Hz, DMSO d_6): δ = 0.83 (t, 3 H), 1.21 (m, 18 H), 1.69 (m, 2 H), 1.16 (t, 2H) 6.85 (t, 1H), J = 8.4 Hz 7.12 (d, 1 H), J = 8.7 Hz, 7.85 (t, 1 H) J = 6.6 Hz 7.95 (d, 1 H) J = 6.3 Hz 8.59 (bs, $-NH_2$, 2 H).

^{13}C NMR (75 MHz, DMSO-d_6): 14.36, 22.53, 25.79, 27.81, 29.07, 29.15, 29.31, 29.37, 29.45, 31.73, 53.42, 113.30, 115.22, 140.45, 142.54, 153.92.

2.3. Synthesis of silver nanoparticles

In typical synthesis 0.1 g 2-amino (do-decyl) pyridinium bromide was dissolved in 10 mL distilled water in an Erlenmeyer flask. To this solution 1 mmole silver nitrate aqueous solution was added and the whole solution stirred for 10 min. After 10 min of mixing of both these solution, 1 mL dilute hydrazine hydrate was added. The solution turns pale yellow to yellow brown in color, indicating formation of silver nanoparticles. A slight excess of hydrazine hydrate was added to confirm complete reduction. The silver nanoparticles were stabilized by reverse micelle system $AgNO_3$/Water/IL and the product was collected by centrifugation. Reaction conditions were optimized by checking the stability and particle size of SNPs.

The synthesis of silver nanoparticles was confirmed by UV-Visible spectroscopy. The UV-Visible spectra shows a surface plasmon resonance (SPR) at about 420 nm. The UV-Visible spectrum of Water/IL system and IL stabilized silver nanoparticles was recorded. Only IL stabilized silver nanoparticles show SPR indicating formation of SNPs. The kinetic study of reaction time at fixed Ag+ and IL concentration were recorded. All UV-Visible analysis was carried out with Shimadzu UV-Visible NIR spectrophotometer (model-3600). Distilled water was used as blank.

Particle size of synthesized silver nanoparticles was analyzed through photon correlation spectroscopy. Light scattering measurements were carried out at 90°, on a photon correlation spectrometer (PCS)–Zetasizer 3000 HAS equipped with a digital autocorrelation from Malvern Instrument UK. The transmission electron diffraction (selected area electron diffraction [SAED]) pattern was taken for morphological analysis of nanoparticles with JEOL-3010 field emission electron microscope with accelerating voltage of 300 kV. The samples were analyzed by preparing a dilute solution in distilled water, drop casted

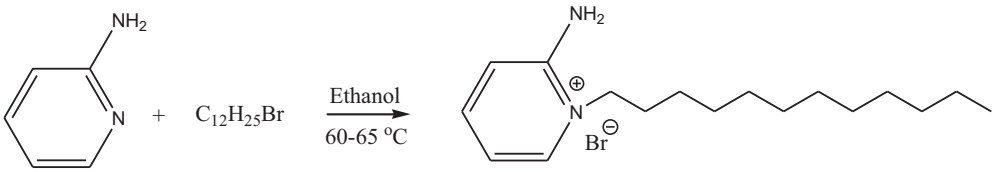

Scheme 1.

Fig. 1. (a) Ionic liquid stabilized silver nanoparticles. (b) Ionic liquid.

on a carbon coated copper grid, followed by drying the sample at ambient conditions before it was attached to the sample holder on the microscope. Particle size distribution (PSD) of same sample after 10 months shows no change in particle size which indicates the particles were more stable and do not agglomerate.

2.4. Bactericidal activity (antimicrobial activity)

Three different groups of bacteria *Escherichia coli* (gram negative bacteria) *Staphylococcus aureus* (gram positive bacteria), and *Pseudomonas aeruginosa* (non ferment gram negative bacteria) were investigated in this study. Nutrient agar and type-I agar were used as media to grow bacteria. The bacterial strains were stored in refrigerator. The bacterial solutions were prepared in 0.86% saline. The antibacterial activity of silver nanoparticle was assayed by following standard Nathan's agar well diffusion technique [31]. The bacterial suspension was spread on nutrient agar in petri plates to create confluent lawn of bacterial growth. The wells of 6 mm were prepared by a borer. The solutions of different concentration (10, 15 and 20 μl) were poured into each well. The well without silver nanoparticles was treated as control. These plates were incubated to 24 h at 35 °C. The lowest concentration at which the petri plate did not show any visible growth after microscopic evaluations was considered as the minimum inhibitory concentration (MIC). The susceptibility of test organisms was determined

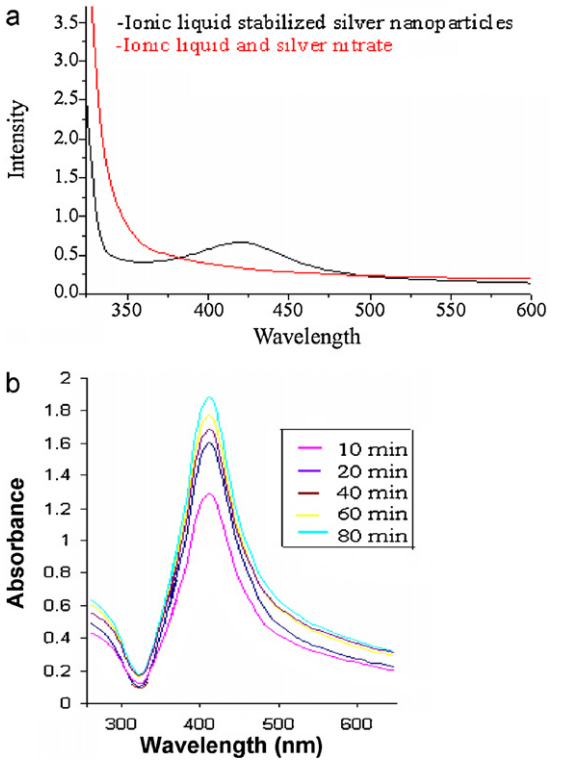

Fig. 3. (a) UV-Visible spectra of water-IL micro emulsion and IL stabilized SNPs. (b) Kinetics of formation of SNPs from UV-Visible study.

after 24 h by measuring the zone of inhibition around each well to the nearest mm. The results of antimicrobial activity were compared with the control experiment. The control is having 0.1 g IL and 10 mL water (10 μl is used in actual experimentation). This is the same as that used in the synthesis of silver nanoparticles. No zone of inhibition was observed; indicating that the antimicrobial activity is due to IL stabilized SNPs and not due to the IL. All antimicrobial parameters have been studied in triplicate.

3. Results and discussion

Colloidal dispersion of SNPs was successfully prepared by the reduction of silver nitrate by hydrazine hydrate in water ionic liquid micro emulsion. Water-IL micro emulsion containing Ag+ ions is slowly turned brownish yellow in color within 2 h after the hydrazine hydrate

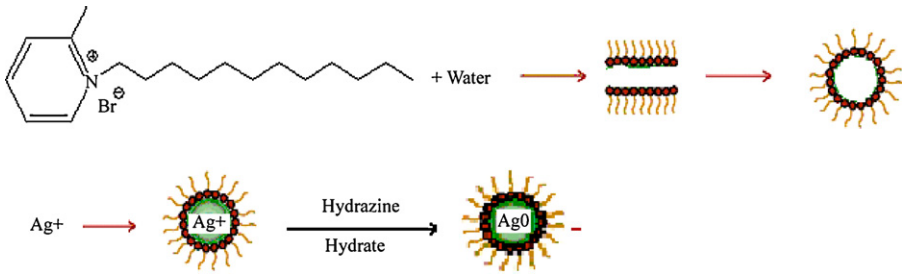

Fig. 2. Schematic illustration of probable formation of silver nanoparticles.

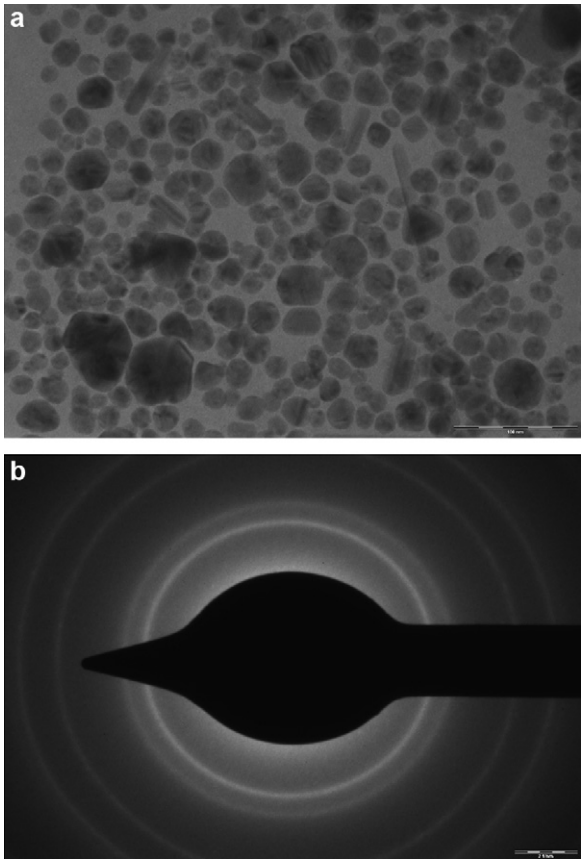

Fig. 4. (a) TEM micrograph of IL stabilized silver Nan particles (SNPs). (b) SAED pattern of IL stabilized SNPs.

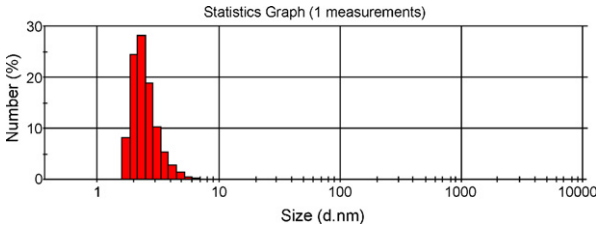

Fig. 5. Particle size distribution of IL stabilized silver Nan particles (SNPs) showing histogram.

reduction was started. The micro emulsion phase containing SNPs was highly dispersed in water IL phase. Fig. 1 shows samples of ionic liquid and IL stabilized SNPs.

Fig. 2 shows a schematic representation of the possible formation of SNPs. The water-IL phase shows clear micro emulsion; it consists of micelle. This micelle will trap the Ag+ ions from aqueous solution of $AgNO_3$. The reduction of Ag+ ions to Ag^0 takes place by hydrazine hydrate. This is indicated by the color change from colorless to yellowish brown. This color arises due to surface plasmon vibrations of metal nanoparticles.

Fig. 3a shows UV-Visible spectra of water IL micro emulsion and IL stabilized silver nanoparticles. The IL stabilized SNPs shows SPR at 430 nm indicating formation of silver nanoparticles. The kinetics of reduction reaction can be studied from UV-Visible spectroscopy. Fig. 3b shows UV-Visible measurements at various time intervals that are at 10, 20, 40, 60 and 80, at 60 and at 80 min. Thereafter there is no increase in peak intensity indicating completion of reaction.

Further, to get closer insight into SNPs formation, some kinetic parameter can be evaluated. From kinetic point of

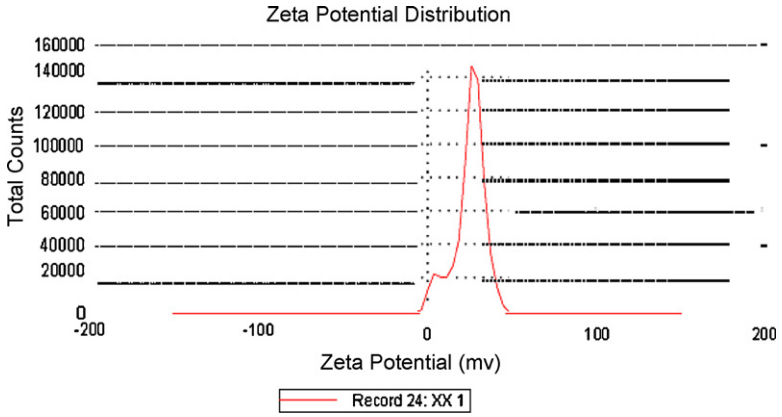

Fig. 6. Zeta potential measurement of IL stabilized silver Nan particles (SNPs).

Table 1
The results of antibacterial activity with zone of inhibition.

No.	Bacterial strains	Zone of inhibition by silver Nan particles (SNPs)			
		Control (mm)	10 μl (mm)	15 μl (mm)	20 μl (mm)
1	*Escherichia coli*	0	8	12	15
2	*Staphylococcus aureus*	0	10	15	20
3	*Pseudomonas aeruginosa*	0	3	5	11

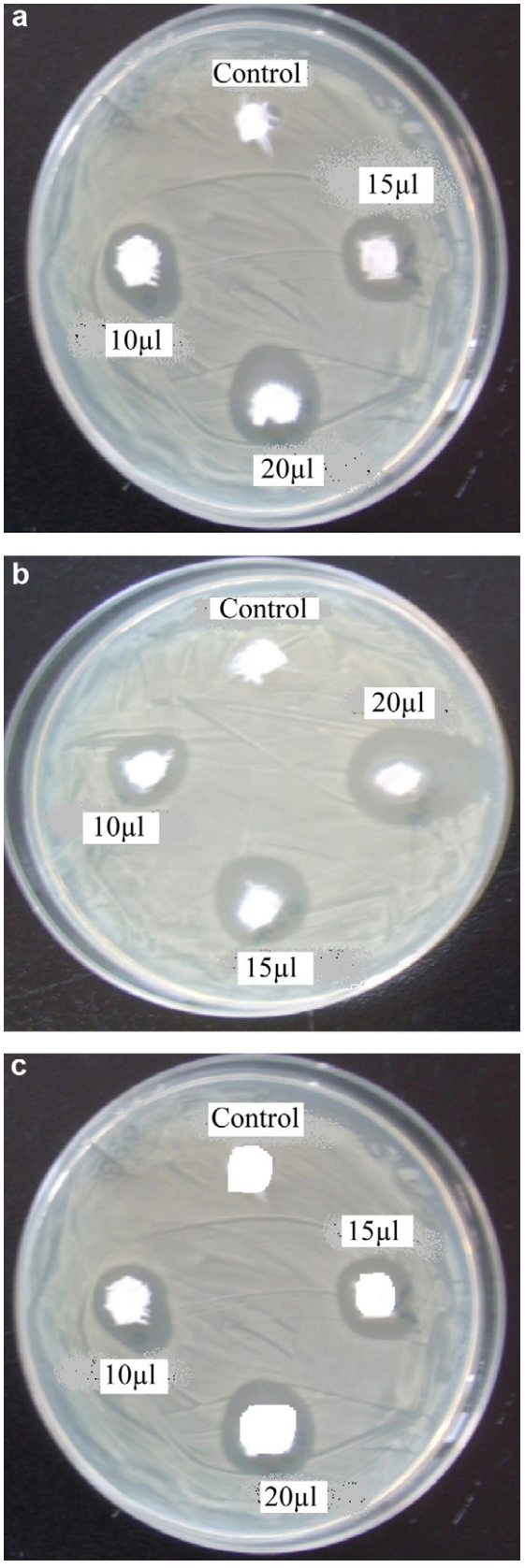

view, Ag+ reduction by hydrazine in water-IL micro emulsion can be described by following equation:

$$\nu = \frac{d[\mathrm{Ag+}]}{dt} = -Kdt = K[\mathrm{Ag+}]^n \quad (1)$$

where K = rate constant, [Ag+] = silver ion concentration and n is the order of reaction. It may be interest to determine the order of reduction reaction that the variation of time at constant silver ion concentration and water-IL micro emulsion concentration. The dependence of adsorption A on concentration C can be represented by Lambert-Beer equation:

$$A = \varepsilon(\lambda)/c \quad (2)$$

where A = absorption, l = path length, λ = monochromatic wavelength, ε = molar extinction coefficient. It should be emphasized that linear correlation between A and C in the Lambert-Beer equation is valid only for diluted solution. Lambert-Beer equation therefore can be applied and rearranged for more convenient monitoring by UV-Visible measurements.

$$\ln[Ag^+]_t/[Ag^+]_0 = \ln[Ag^0]_\infty - [Ag^0]_t/[Ag^0]_\infty = \ln A_\infty - At/A_\infty = -kt \quad (3)$$

where $[Ag^+]_o$, $[Ag^+]_t$, $[Ag^0]_\infty$ describe silver ion concentration at initial time ($t = 0$), at a moment t during reaction time and at final time ($t = \infty$) respectively. A_t and A_∞ are the absorbance values at respective moment.

From equation (3) linear logarithmic ln $A_\infty - A_t/A_\infty$ vs plot performs that Ag^+ reduction reaction obeys first order kinetics.

Fig. 4a and b show TEM and SAED images of synthesized IL stabilized SNPs. The morphology of nanoparticles is highly variable with spherical and occasionally rod like nanoparticles observed on the micrograph. The TEM micrograph suggests that particle diameter ranged from 2 to 20 nm. The scale bar is 100 nm. The selected area electron diffraction pattern shows the particles were highly crystalline with zero valent FCC silver, representing (111), (200), (220), and (311) crystal planes and aggregation of each particle does not noticeably occur.

Fig. 5 shows PSD of histogram of colloidal dispersion of SNPs. The PSD shows particles are distributed in between 2 to 10 nm. Fig. 6 shows the zeta potential of IL stabilized silver nanoparticles to be 24.6 eV. This shows that particles were having positive charge on their surface.

The antibacterial activity of synthesized hybrid materials against etalon strains of three different groups of bacteria *E. coli* (gram negative bacteria), *S. aureus* (gram positive bacteria) and *P. aeruginosa* (non ferment gram negative bacteria) has been studied. The results of antibacterial activity with zone of inhibition are tabulated in Table 1. The MIC is 10 µl. Control shows no zone of inhibition, this indicates the antimicrobial activity is due to IL stabilized SNPs. Fig. 7a, b and c antibacterial effect of

Fig. 7. (a) Antimicrobial effect of Silver nanoparticles on *Escherichia coli*. (b) Antimicrobial effect of silver nanoparticles on *Staphylococcus aureus*. (c) Antimicrobial effect of Silver nanoparticles on *Pseudomonas aeruginosa*.

E. coli, *S. aureus* and *P. aeruginosa*. *E. coli* shows zones of inhibition of 8, 12 and 15 mm. *S. aureus* shows zones of inhibition of 10, 15 and 20 mm and *P. aeruginosa* shows zones of inhibition of 3, 5 and 11 mm for 10, 15 and 20 μl, respectively. This vast difference may be due to the susceptibility of the organism used in the present study. The maximum antibacterial activity was recorded for *S. aureus*. These results can be interpreted on the basis of the possible mechanisms, all emphasizing the dependence of bacterial action of SNPs on their size, dose, and morphology. Effectively, different mechanisms for bacterial action of SNPs are the following: (i) Ag+ ions are supposed to bind to sulfhydryl groups, which lead to protein denaturation by the reduction of disulfide bonds; (ii) Ag+ can complex with electron donor groups containing sulfur, oxygen, or nitrogen that are normally present as thiols or phosphates on amino acids and nucleic acids. Also, SNPs have been found to attach to the surface of the cell membrane and disturb its function, penetrate bacteria, and release Ag; (iii) SNPs target the bacterial membrane, leading to a dissipation of the proton motive force. Thus, a decrease in the SNPs size can lead to an increase in the specific surface of a bactericidal specimen, inducing an increase in their ability to penetrate cell membrane, and thus improving antibacterial activity. It has also been reported that SNPs with size range of 1–10 nm attach to cell membrane and drastically disturb its proper function, like permeability and respiration, further on penetration, more damage is caused by interacting with sulfur and phosphorous containing compounds like DNA.

The higher antibacterial activity against *S. aureus* is probably driven by the difference in the structure of cell walls between gram-negative and gram-positive bacteria. The cell wall of gram-negative bacteria consists of lipids, proteins and lipopolysaccharides (LPS) that ensure more effective defense against biocides in comparison to gram-positive bacteria where the cell wall does not contain an outer membrane of LPS [32,33] thus leading to the higher antibacterial activity of the IL stabilized silver nanoparticle. It should be noted that an insignificant difference is observed in the size of the inhibition zones with increasing the silver concentration from 10, 15 and 20 μl.

The bactericidal activity is presumably due to certain changes in the membrane structure of bacteria cell wall as a result of the interaction with the embedded SNPs which leads to the increased membrane permeability of the bacteria and consequently, leading to their death [34].

4. Conclusion

In summary, the synthesis and kinetics of silver reduction by hydrazine hydrate in a water-IL micro emulsion were investigated. The ionic liquid itself can act as an electronic as well as steric stabilizer and depress particle growth. The highly structured ILs have strong effect on the morphology of particles formed. The appropriate concentration of IL can effectively produce finely dispersed SNPs with average size distribution of 2–20 nm. Silver nanoparticles exhibit excellent antibacterial activity against three bacterial strains *S. aureus, E. coli. P. aeruginosa*. These enhanced activities can be explained by the fact that silver nanoparticles are monodispersed to attach to the surface of cell and penetrate through the cell membrane which could make SNPs promising candidates for many biomedical applications.

Acknowledgement

One of the author (RSP) is grateful to the Department of Chemistry, Shivaji University, Kolhapur and University Grants Commission, New Delhi for SAP Fellowship. We are also grateful to the Department of Science and Technology, Government of India for DST-FIST programme facilities, Indian Institute of Technology, Mumbai for TEM characterization.

References

[1] K.S. Kim, S. Choi, D. Demberelnyamba, H. Lee, J. Oh, B.B. Lee, S.J. Man, Chem. Commun. 2 (2004) 828.
[2] D.R. Mac Farlane, J. Huang, M. Forsyth, Nature 402 (1999) 792.
[3] J. Dupont, G.S. Fonseca, A.P. Umpierre, P.F.P. Fichtner, S.R. Teixeira, J. Am. Chem. Soc. 124 (2002) 4228.
[4] K.S. Kim, D. Demberelnyamba, H. Lee, Langmuir 20 (2004) 556.
[5] K.S. Kim, D. Demberelnyamba, S.H. Yeon, S. Choi, J.H. Cha, H. Lee, Korean J. Chem. Eng. 22 (2005) 717.
[6] K. Binnemans, Chem. Rev. 105 (2005) 4148.
[7] J. Ding, D.W. Armstrong, Chirality 17 (2005) 281.
[8] P. Wasserstein, T. Welton (Eds.), Ionic liquid in synthesis, Wiley VCH Verlag GmbH and Co. KGaA, Weinheim, 2003.
[9] Y. Wang, H. Yang, J. Am. Chem. Soc. 127 (2005) 5316.
[10] C.C. Cassol, A.P. Umpierre, G. Machedo, S.I. Wolke, J. Dupont, J. Am. Chem. Soc. 127 (2005) 3298.
[11] K. Chokshi, S. Qutubuddin, A. Hussam, J. Colloid Interf. Sci. 129 (1989) 315.
[12] D.I. Gittins, D. Bethell, D.J. Schiffrin, R.J. Nichols, Nature 408 (2000) 67.
[13] P. Mukherjee, M. Roy, B.P. Mandal, G.K. Dey, P.K. Mukherjee, J. Ghatak, A.K. Tyagi, S.P. Kale, Nanotechnology 19 (2008) 075103.
[14] Y.G. Sun, B. Mayers, T. Herricks, Y.N. Xia, Nano. Lett. 3 (2003) 955.
[15] Y.N. Xia, N.J. Halas, MRS Bull. 30 (2005) 338.
[16] P. Raveendran, J. Fu, S.L. Wallen, Green Chem. 8 (2006) 34.
[17] Y. Shiraishi, D. Arakawa, N. Toshima, Eur. Phys. J. E. 8 (2002) 377.
[18] D.K. Bhui, H. Bar, P. Sarkar, G.P. Sahoo, S.P. De, A. Misra, J. Mol. Liquids 145 (2009) 33.
[19] W. Songping, M. Shuyuan, Mater. Chem. Phys. 89 (2005) 423.
[20] C.N. Lok, C.M. Ho, R. Chen, Q.Y. He, W.Y. Yu, H. Sun, P.K. Tam, J.F. Chiu, C.M. Chen, J. Proteome. Res. 5 (2006) 916.
[21] C. Baker, A. Pradhan, L. Pakstis, D.J. Pochan, S.I. Shah, J. Nanosci. Nanotechol. 5 (2005) 244.
[22] C. Aymonier, U. Schlotterbeck, L. Antonietti, P. Zacharias, R. Thomann, J.C. Tiller, S. Mecking, Chem. Commun. 24 (2002) 3018.
[23] A. Melaiye, Z. Sun, K. Hindi, A. Milsted, D. Ely, D.H. Renekar, C.A. Tessier, W.J. Youngs, J. Am. Chem. Soc. 127 (2005) 2285.
[24] I. Sondi, B. Salopek-Sondi, J. Colloid Interface. Sci. 275 (2004) 177.
[25] K.J. Kim, W.S. Sung, S.K. Moon, J.S. Choi, J.G. Kim, D.G. Lee, J. Microbiol. Biotechnol. 18 (8) (2008) 1482.
[26] B.U. Lee, S.H. Yun, J.H. Ji, G.N. Bae, J. Microbiol. Biotechnol. 18 (2008) 176.
[27] V. Alt, T. Bechert, P. Steinrucke, M. Wagner, P. Seidel, E. Dingeldein, E. Domann, R. Schnettlet, Biomaterials 25 (2004) 4383.
[28] V. Thomas, M.M. Yallupu, B. Sreedhar, S.K. Bajpai, J. Colloid Interface Sci. 315 (2007) 389.
[29] S. Kim, H.J. Kim, Int. Biodeterioration Biodegradation 57 (2006) 155.
[30] U. Lad, S. Khokhar, G.M. Kale, Anal. Chem. 80 (2008) 7910.
[31] P. Nathan, E.J. Law, D.F. Murphy, Burns 4 (1978) 177.
[32] T. Maneerung, T. Seiichi, R. Rujiravanit, Carbohydr. Polym. 72 (2008) 43.
[33] Q. Feng, J. Wu, G.Q. Chen, F.Z. Cui, T.N. Kim, J.O. Kim, J. Biomed. Mater. Res. 5 (2000) 662.
[34] P. Dibrov, J. Dzioba, K.K. Gosink, C.C. Hase, Antimicrob. Agents Chemother. 46 (2002) 2668.